Installation Effects in Geotechnical Engineering – Hicks et al. (eds)
© 2013 Taylor & Francis Group, London, ISBN 978-1-138-00041-4

Coupling triangular plate and volume elements in analysis of geotechnical problems

S. Tan
Geo-Engineering Section, Faculty of CITG, Delft University of Technology, Delft, The Netherlands

M.A. Hicks
Geo-Engineering Section, Faculty of CITG, Delft University of Technology, Delft, The Netherlands
Deltares, Delft, The Netherlands

A. Rohe
Deltares, Delft, The Netherlands

ABSTRACT: In geotechnics, it is common to have a thin layered material with high stiffness on top of soil, to prevent damage from external loading or erosion. To model this numerically a very fine mesh is often needed, which decreases the critical time step in explicit time integration algorithms, severely affecting simulation performance. The use of 2D plate elements connected to 3D elements is investigated to overcome this problem. The presented three-noded plate element is based on Kirchhoff thin plate theory, and uses non-conforming polynomial shape functions. The lumped mass matrix, with both the translational and rotational degrees of freedom considered, is implemented with an explicit time integration scheme. This plate element is coupled with volume elements and the implementation is tested for several cases in which analytical or numerical solutions are available. All simulations show that the plate element with the lumped mass matrix is working properly in geotechnical problems.

1 INTRODUCTION

The plate bending problem was one of the first problems to which the Finite Element Method was applied in the early 1960s. A three-noded triangular plate bending element with nine degrees of freedom was first derived by Bazeley et al. (1965), based on Kirchhoff thin plate theory. Although it satisfies the constant strain criterion, it unfortunately does not pass the test for arbitrary mesh configurations (Batoz et al., 1980). However, Specht (1988) proposed a successful modification procedure, which passes the test perfectly by using three fourth-order terms in the plate polynomial function.

In order to analyze dynamic problems, the explicit time integration procedure is often used, which has been extensively developed for dynamic analyses to meet the increasing demand of geotechnical applications. Moreover, the consistent mass matrix is well established, but it requires a considerable computational cost and storage effort. The use of a lumped mass matrix simplifies the program coding and significantly reduces the computational requirements. However, for plate elements with both translational and rotational degrees of freedom, it has been customary to construct the lumped mass matrix by neglecting the inertia effects of the rotational degrees of freedom (Surana, 1978; Batoz et al., 1980). Unfortunately, this can lead to low accuracy results, especially when solving geotechnical problems with the combination of plate elements and volume elements.

Therefore, a lumped mass matrix, considering both the translational and rotational degrees of freedom, is introduced for the three-noded triangular plate element. The modified non-conforming shape functions based on area coordinates are explained in detail, and the lumped mass matrix for the plate element is derived without neglecting the rotational degrees of freedom. Based on the plate theory, the explicit time integration procedure for dynamic analysis is presented. By assembling the plate and volume elements in a 3D code, the plate elements can be used to model a thin layer material instead of volume elements.

For validation purposes, the implementation is tested for several cases in which analytical solutions or numerical results are available. 2D problems of a square cantilever plate and a circular plate are considered, followed by a plane strain problem of a plate resting on an elastic foundation and a cir-

cular concrete plate resting on a homogeneous half space. Finally, the conclusions are provided.

2 METHODOLOGY

Kirchhoff plate theory is an extension of the Euler-Bernoulli beam theory for thin plates. It uses the mid-surface plane to represent the three dimensional plate in a two dimensional form.

The fundamental assumptions are that straight lines normal to the mid-surface are infinitely rigid and that, after deformation, they remain straight and normal to the mid-surface (Reddy, 2007; Bauchau & Craig, 2009). Experimental measurements show that these assumptions are valid for thin plates made of homogeneous, isotropic materials. All the equations are based on these assumptions.

2.1 *Shape functions with area coordinate system*

For the three-noded triangular plate element, three degrees of freedom (one deflection and two rotations) at each vertex are used as nodal variables. The nodal displacement vector at node i can be defined as $\mathbf{a}_i$. The element displacement will therefore be given by a listing of nine nodal displacements, i.e.

$$\mathbf{a}^e = \begin{Bmatrix} \mathbf{a}_i \\ \mathbf{a}_j \\ \mathbf{a}_k \end{Bmatrix}, \quad \mathbf{a}_i = \begin{Bmatrix} w_i \\ \theta_{xi} \\ \theta_{yi} \end{Bmatrix} \tag{1}$$

in which w_i is the deflection of the node; and θ_{xi} and θ_{yi} are the rotations relative to the x- and y-axes of the plate, respectively, and are defined as,

$$\theta_{xi} = -\left.\frac{\partial w}{\partial y}\right|_i, \quad \theta_{yi} = -\left.\frac{\partial w}{\partial x}\right|_i \tag{2}$$

The continuous displacement variable, in this case the deflection w, is approximated in terms of discrete nodal values as follows,

$$w \approx \mathbf{N}\mathbf{a}^e = [\mathbf{N}_i \;\; \mathbf{N}_j \;\; \mathbf{N}_k][\mathbf{a}_i^{\mathrm{T}} \;\; \mathbf{a}_j^{\mathrm{T}} \;\; \mathbf{a}_k^{\mathrm{T}}]^{\mathrm{T}} \tag{3}$$

where $\mathbf{N}$ is the matrix of shape functions derived by Specht (1988), given by,

$$\mathbf{N}_i^{\mathrm{T}} = \begin{Bmatrix} P_i - P_{i+3} + P_{k+3} + 2(P_{i+6} - P_{k+6}) \\ -b_j(P_{k+6} - P_{k+3}) - b_k P_{i+6} \\ -c_j(P_{k+6} - P_{k+3}) - c_k P_{i+6} \end{Bmatrix} \tag{4}$$

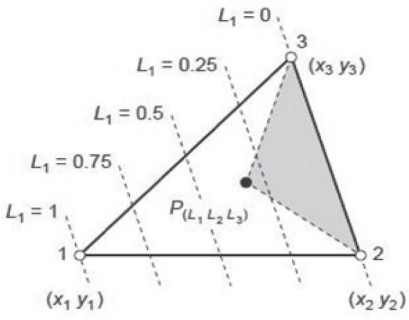

Figure 1. Area coordinates of triangular element.

where $b_i = y_j - y_k$, $c_i = x_k - x_j$; x and y are the coordinates of the nodes (Figure 1); i, j, k are cyclic permutations of 1, 2, 3; and $\mathbf{P}$ is the polynomial expression used to define the shape functions in terms of nine parameters,

$$\begin{aligned} \mathbf{P} = [&L_1,\ L_2,\ L_3,\ L_1L_2,\ L_2L_3,\ L_3L_1, \\ &L_1^2L_2 + \frac{1}{2}L_1L_2L_3\{3(1-\mu_3)L_1 - (1+3\mu_3)L_2 + (1+3\mu_3)L_3\}, \\ &L_2^2L_3 + \frac{1}{2}L_1L_2L_3\{3(1-\mu_1)L_2 - (1+3\mu_1)L_3 + (1+3\mu_1)L_1\}, \\ &L_3^2L_1 + \frac{1}{2}L_1L_2L_3\{3(1-\mu_2)L_3 - (1+3\mu_2)L_1 + (1+3\mu_2)L_2\}] \end{aligned} \tag{5}$$

where μ_i is defined as,

$$\mu_i = \frac{l_k^2 - l_j^2}{l_i^2} \tag{6}$$

and l_i is the length of the triangle side opposite to node i (Figure 2).

L_1, L_2 and L_3 are the area coordinates, which are defined by the following linear relationship with the Cartesian system,

$$\begin{aligned} x &= L_1x_1 + L_2x_2 + L_3x_3 \\ y &= L_1y_1 + L_2y_2 + L_3y_3 \\ 1 &= L_1 + L_2 + L_3 \end{aligned} \tag{7}$$

The coordinate L_1 of a point P is defined as the ratio of the area of the shaded triangle to that of the entire triangle, i.e.

$$L_1 = \frac{\text{area } P23}{\text{area } 123} \tag{8}$$

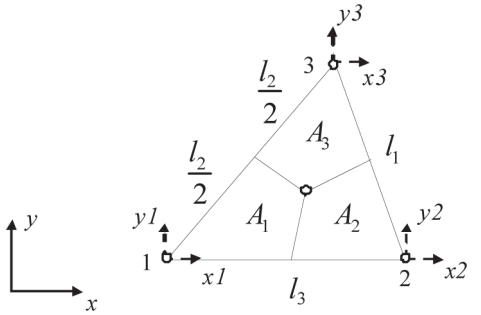

Figure 2. Mass lumping for 3-node triangular plate element.

2.2 *Lumped mass matrix*

The lumped mass matrix is built up by mapping the mass of the surrounding elements to the respective nodes of the elements. Considering the three degrees of freedom of each node, the construction of the mass matrix consists of two different types of terms. For the translational degree of freedom, it is equivalent to the normal mass matrix. The mass of the element is divided into three parts by the central point of the element (Figure 2). Each node in the element carries 1/3 of the total mass (m) and it goes to the term for the translational degree of freedom.

In classical mechanics, the moment of inertia is the property of a mass in space that measures its resistance to rotational acceleration around an axis. It plays the same role in rotational motion as mass does in translational motion, describing the relationship between the moment of momentum and angular velocity, torque and angular acceleration. Therefore, the moment of inertia (J) is used for the terms of the rotational degree of freedom. It is calculated in the local coordinate system of each node, as shown in Figure 2. Therefore, the diagonal terms of the mass matrix are,

$$\mathbf{M}_L = \left[\frac{m}{3} \;\; J_{x1} \;\; J_{y1} \;\; \frac{m}{3} \;\; J_{x2} \;\; J_{y2} \;\; \frac{m}{3} \;\; J_{x3} \;\; J_{y3} \right] \quad (9)$$

where the moments of inertia can be defined as,

$$\begin{aligned} J_{x1} &= \iint_{A_1} \rho {y_1}^2 dx_1 dy_1, \quad J_{y1} = \iint_{A_1} \rho {x_1}^2 dx_1 dy_1 \\ J_{x2} &= \iint_{A_2} \rho {y_2}^2 dx_2 dy_2, \quad J_{y2} = \iint_{A_2} \rho {x_2}^2 dx_2 dy_2 \\ J_{x3} &= \iint_{A_3} \rho {y_3}^2 dx_3 dy_3, \quad J_{y3} = \iint_{A_3} \rho {x_3}^2 dx_3 dy_3 \end{aligned} \quad (10)$$

where A_i indicates the area related to node i in an element, as shown in Figure 2.

2.3 *Equations of motion in dynamic analysis*

Considering a dynamic process using an explicit time integration scheme, the discrete equation of motion can be written as,

$$\mathbf{M}_L \ddot{\mathbf{w}} = \mathbf{F}^{ext} - \mathbf{F}^{int} \quad (11)$$

where $\mathbf{w}$ is the displacement vector, which includes deflections and rotations; $\mathbf{M}_L$ is the lumped mass matrix of the plate element; $\mathbf{F}^{ext}$ is the nodal external force vector, including the external traction and body forces; and $\mathbf{F}^{int}$ is the nodal internal force vector resulting from the bending and torsion moments. The internal force vector is given by,

$$\mathbf{F}^{int} = \int_S \mathbf{B}^T \mathbf{M} dS \quad (12)$$

where S is the area of the element, and $\mathbf{M}$ is the element bending moment vector, which contains M_{xx}, M_{yy} and M_{xy}. It is calculated as,

$$\mathbf{M} = \mathbf{D}\mathbf{B}\mathbf{a}^e \quad (13)$$

in which $\mathbf{B}$ is the matrix of the second derivative of the shape functions, namely,

$$\mathbf{B} = \left[\frac{\partial^2}{dx^2} \;\; \frac{\partial^2}{dy^2} \;\; 2\frac{\partial^2}{dxdy} \right]^{\mathrm{T}} \left[\mathbf{N}_i \;\; \mathbf{N}_j \;\; \mathbf{N}_k \right] \quad (14)$$

and $\mathbf{D}$ is called the "flexural rigidity" which is analogous to the bending stiffness EI of a beam, i.e.

$$\mathbf{D} = \begin{bmatrix} D & \nu D & 0 \\ \nu D & D & 0 \\ 0 & 0 & \dfrac{(1-\nu)D}{2} \end{bmatrix}, \quad D = \frac{Et^3}{12(1-\nu^2)} \quad (15)$$

where t is the thickness of the plate and ν is Poisson's ratio.

In order to reach an the equilibrium state for the dynamic problem, the local damping is introduced as defined in FLAC (1998) by adding an artificial damping term into equation (11), i.e.

$$\mathbf{M}_L \ddot{\mathbf{w}} = \mathbf{F}^{ext} - \mathbf{F}^{int} - \mathbf{F}^{damping} \quad (16)$$

in which $\mathbf{F}^{damping}$ is the damping force vector. Its components are defined as,

$$F_i^{damping} = \alpha \left| F_i^{ext} - F_i^{int} \right| \text{sign}(\dot{w}_i), \quad i=1,2,\ldots N_{dof} \tag{17}$$

where α is the damping factor and N_{dof} is the total number of degrees of freedom.

3 NUMERICAL SIMULATIONS OF 2D PROBLEMS

The plate element presented above has been implemented in a 3D code and coupled with tetrahedral elements for representing the underlying soil. The implementation has been tested for both 2D and 3D cases in which analytical or numerical solutions are available for validation.

3.1 *Cantilever square plate*

The plate element was first tested for a 2D problem; this being the modelling a square plate, clamped at one end and subjected to a vertical line load at the free end, as shown in Figure 3. The plate has a thickness of 0.01 m. The material is considered to be linear elastic, with a Young's modulus E = 180GPa, Poisson's ratio ν = 0, and density ρ = 1000 kg/m^2. The magnitude of the lateral distributed load is assumed to be 2 kN/m.

Three finite element meshes have been considered and the deflection of the corner point B for each mesh is listed in Table 1, along with the analytical result. As can be seen in Table 1, the calculation error reduces to almost zero with increasing number of elements, indicating that the plate element performs well.

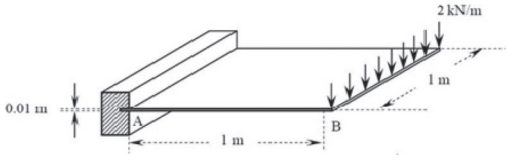

Figure 3. Cantilever plate subjected to a uniform end load.

Table 1. Comparison of results for deflection of Point B.

	Deflection (m)	Analytical result (m)	Error
4 elements	0.0433		2.47%
8 elements	0.0437	0.0444	1.58%
12 elements	0.0442		0.45%

3.2 *Circular plate with simply supported edge*

Figure 4 shows a simply supported circular plate with a point load applied at its centre. The plate is modelled as linear elastic, with a Young's modulus E = 200 MPa, and Poisson's ratio ν = 0. The radius of the plate is a = 0.45 m and the thickness is t = 0.1 m. The applied point load is q = 10 kN.

The analysis has been done using a local damping factor of 0.5 to reach the equilibrium state. Figure 5 shows the deflection of the loaded point as a function of time, with the final deflection of 7.24 mm being in close agreement to the analytical solution of 7.25 mm. Figure 6 shows the contour plot of the deflection of the plate.

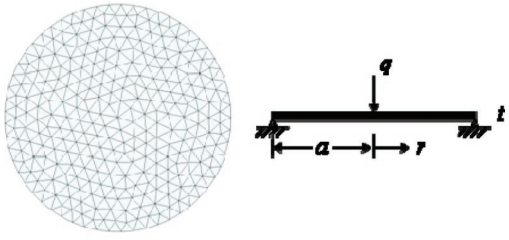

Figure 4. Geometry of circular plate: a. elevation of the mesh; b. side view.

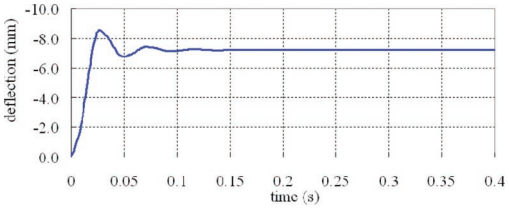

Figure 5. Plot of deflection of the loaded point.

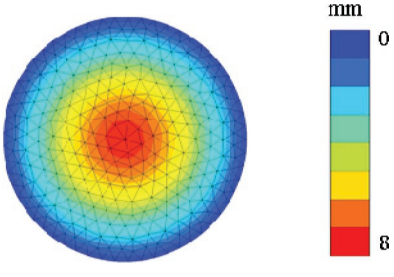

Figure 6. Contour plot of deflection of the circular plate.

4 NUMERICAL SIMULATIONS OF 3D PROBLEMS

In order to solve the problem of a thin layered material resting on soil, the 2D plate element has been implemented in a 3D finite element code which uses tetrahedral elements for modelling the soil volume. In this case, the assembling nodes share information of both the plate element and tetrahedral element, with five degrees of freedom, three for translation and two for rotation. Because of the different shape functions of the plate and volume elements, the continuity equation is only applied to the vertical displacements of the nodes, which belong to both types of element.

4.1 *Plate resting on elastic foundation*

A plate resting on an elastic foundation has been considered by using the 3D code to model what is a plane strain problem, as shown in Figure 7. The plate has a virtual thickness of 0.05 m, and a uniform load of $p = 12$ kN/m^2 has been applied to the middle area of the plate over a width of 0.1 m. Both the plate and soil are modelled as linear elastic, with the Young's modulus for soil being 2000 kN/m^2 and for the plate 20000 kN/m^2, and with both having a Poisson's ratio of 0.0. The dimensions of the problem are shown in Figure 7.

As expected, the highest stresses and displacements are concentrated just below the loaded area, as indicated in Figures 8 and 9, respectively. For comparison, the same problem has been analyzed by the Plaxis 2D code using Mindlin plate elements. Similar results are obtained for both the stresses (Figure 8b) and displacements (Figure 9b), although the values from Plaxis are slightly higher than those from the 3D code. However, although the two meshes are similar, Plaxis 2D uses 6-noded high order elements, while the 3D code uses low order elements, which is likely to be the reason for the slight differences in the results.

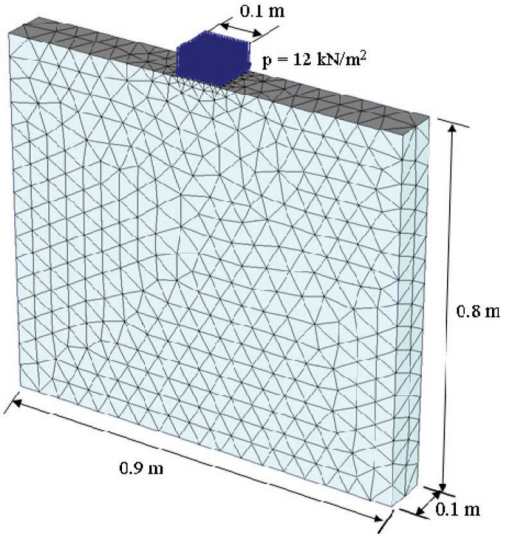

Figure 7. Geometry of centrally loaded plate resting on elastic foundation.

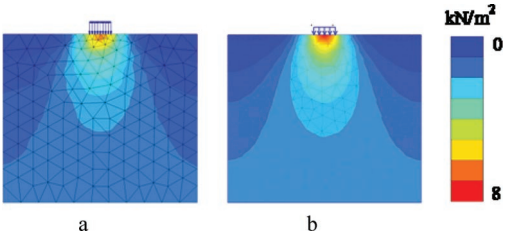

Figure 8. Contour plots of vertical stress in the soil below loaded plate: a. results using implemented plate element; b. results using Plaxis.

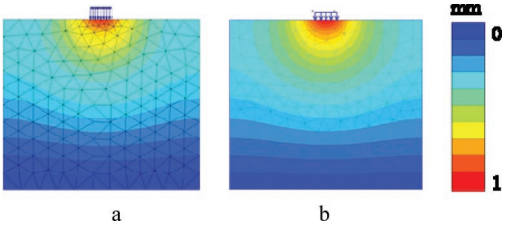

Figure 9. Contour plots of vertical displacement in the soil below loaded plate: a. results using implemented plate element; b. results using Plaxis.

4.2 *Concrete plate resting on elastic soil*

In this subsection, a circular plate has been used to model a concrete layer resting on top of a homogeneous elastic soil layer. The plate is subjected to a load $q = 12$ kN/m^2 applied centrally over a circular area of 10 cm diameter. As shown in Figure 10, the discretized region has a diameter of 90 cm, and a depth of 80 cm. The plate has a virtual thickness of 5 cm.

The soil is idealised as linear elastic, with a Young's modulus of $E_2 = 2000$ kN/m^2 and Poisson's ratio of $\nu = 0.0$. The plate is modelled as linear elastic, with a Poisson's ratio of $\nu = 0.0$. In order to study the interaction between the soil and the plate, different values of Young's modulus are used for the concrete plate, namely, $E_1 = 10000$ kN/m^2, 20000 kN/m^2 and 40000 kN/m^2.

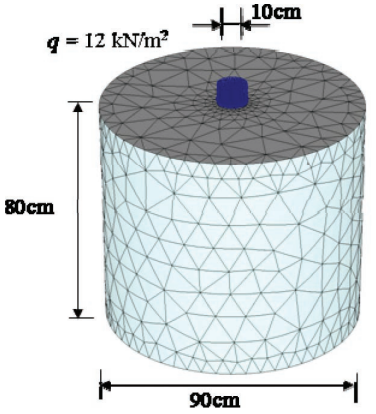

Figure 10. Geometry of loaded plate resting on half space.

This problem can be considered as a two-layer problem. The concrete plate significantly reduces the stresses and deflections in the soil, especially when the modular ratio of the plate and soil (E_1/E_2) is large. Solutions for the two-layer problem have been obtained by Burmister (1945) using strain continuity equations, which indicate the dependency on E_1/E_2. Figure 11 shows the vertical stress ratio below the centre of the circular plate for the two-layer system (Burmister, 1958; Yoder & Witczak, 1975), as a function of E_1/E_2.

After applying the load to the circular area, stresses and deflections are generated in the soil. The soil just below the loaded area experiences the highest stresses, as shown in Figure 12, for the plate with a Young's modulus of $E_2 = 20000$ kN/m^2. The vertical stresses in the soil decrease with depth, but the maximum value occurring at the interface between the plate and soil is equal to 3.33 kPa, which is 27.8% of the applied load. According to Figure 11, for a modular ratio of 10, the vertical stress at the interface of the two layers is approximately 30% of the applied load. As the maximum value obtained in the numerical analysis is computed at the stress point of the volume element just below the loaded area, which means that the parameter z/a in Figure 11 is slightly bigger than 1, the vertical stress is consequently less than 30%. Therefore, the obtained stresses in the numerical analysis are reasonable compared with the analytical results. Figure 13 shows the contour plots of the settlements after loading.

The calculations were also done with plate Young's moduli of 10000 kN/m^2 and 40000 kN/m^2. The maximum vertical stresses occur for both cases at the same stress point as before, with magnitudes of

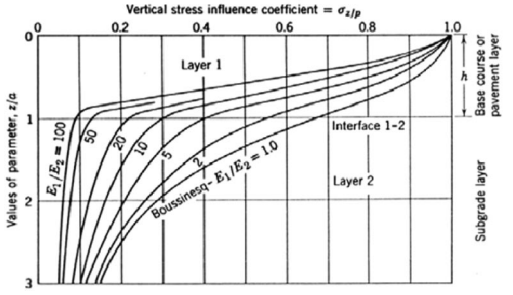

Figure 11. Vertical stresses in a two layer system (Burmister, 1958).

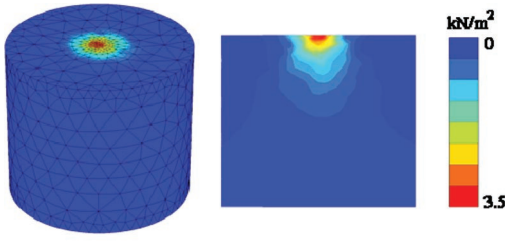

Figure 12. Contour plots of vertical stress: a. 3D view; b. cross section through problem ($E_2 = 20000$ kN/m^2).

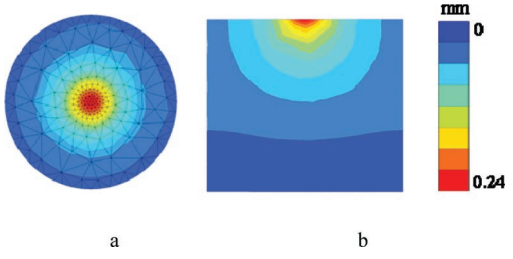

Figure 13. Contour plots of settlement: a. top view; b. cross section through problem ($E_2 = 20000$ kN/m^2).

4.62 kPa and 2.33 kPa, respectively. Once again, there is a good agreement with the theory (Figure 11).

5 CONCLUSIONS

Based on Kirchhoff thin plate theory, the lumped mass matrix of the three-noded triangular plate element has been introduced, considering both the translational and rotational degrees of freedom. In combination with high order non-conforming polynomial shape functions, the explicit time integration scheme was presented for dynamic plate

analysis. The static problems considered in this paper were solved using a transient dynamic procedure with the dynamic relaxation method. Different cases were studied in 2D and 3D, and the results were validated using analytical or numerical solutions. All simulations showed that the lumped mass matrix works properly with the plate element. The plate element can be applied to layered geotechnical problems, to simulate a thin layered material instead of using volumetric elements.

ACKNOWLEDGEMENT

This research is funded by the CSC (China Scholarship Council), TU Delft and Deltares. The authors appreciate the contributions of Professor Vermeer from Deltares, and Professor Wieckowski from Lodz University of Technology and Deltares, who gave valuable advice while doing this research.

REFERENCES

Batoz, J.L., Bathe, K.J. & Ho, L.W. 1980. A study of three-node triangular plate bending elements. *International Journal for Numerical Methods in Engineering*, 15: 1771–1812.

Bauchau, O.A. & Craig, J.I. 2009. *Structural analysis with applications to aerospace structures*. Springer, The Netherlands.

Bazeley, G.P., Cheung, Y.K., Irons, B.M. & Zienkiewicz, O.C. 1965. Triangular elements in plate bending conforming and non-conforming solutions. *Proceedings Conference on Matrix Methods in Structural Mechanics*, Wright Patterson A.F.B., Ohio. 547–576.

Burmister, D.M. 1945. The general theory of stresses and displacements in layered systems. *International Journal of Applied Physics*, 16: 89–94.

Burmister, D.M. 1958. Evaluation of pavement systems of the WASHO road test by layered systems methods. *Highway Research Board Bulletin 177*.

FLAC 1998. Fast lagrangian analysis of continua: theory and background. Itasca Consultin Group, Inc., Minnesota, USA.

Reddy, J.N. 2007. *Theory and analysis of elastic plates and shells*. CRC, Taylor and Francis.

Specht, B. 1988. Modified shape functions for the three-node plate bending element passing the patch test. *International Journal for Numerical Methods in Engineering*, 26: 705–715.

Surana, K.S. 1978. Lumped mass matrices with non-zero inertia for general shell and axisymmetric shell elements. *International Journal for Numerical Methods in Engineering*, 12: 1635–1650.

Yoder, E.J. & Witczak, M.W. 1975. *Principles of pavement design* (2nd Edition). John Wiley & Sons.